Evidence for enhanced desorption of hydrogen atoms from a Si(100) surface induced by slow highly-charged ions

J. Deiwiks[a], G. Schiwietz[b], S.R. Bhattacharyya[c]*, G. Xiao[b], R. Hippler[a]

[a]Institut für Physik, Ernst-Moritz-Arndt-Universität Greifswald,
Domstraße 10a, D-17487 Greifswald, Germany

[b]Hahn-Meitner-Institut Berlin, Glienicker Straße 100, D-14109 Berlin, Germany

[c]Surface Physics Division, Saha Institute of Nuclear Physics,
1/AF Bidhan Nagar, Kolkata 700 064, India

Abstract

We report evidence for an enhanced desorption of hydrogen atoms from a Si(100) surface bombarded by 30 keV Xe^{q+} (q = 6-22) ions. The measured desorption yield amounts to 0.76 and 2.2 hydrogen atoms per incident Xe^{10+} and Xe^{18+} ion, respectively. For understanding the behaviour of hydrogen desorption from Si, another experiment was carried out to see the hydrogen signals as a function of time for about 140 minutes after deliberately introducing hydrogen into the target chamber and then shut off the valve. The results are discussed in the light of *potential sputtering* which essentially dominates for ions at higher charge states and the interpretation is supported by theoretical estimates.

PACS: 79.20 Rf. 79.20 Ne. 79.90 +b

Key words: Desorption, Hydrogen, Highly charged ions, Xenon, Electronic sputtering

*Corresponding author: Tel.: +91-33-23375345, FAX: +91-33-23374637;

e-mail: satyar.bhattacharyya@saha.ac.in

1. Introduction

Various new effects occur during the bombardment of solid surfaces with highly-charged ions (HCI), for example, an increased erosion of the surface caused by the large potential energy carried by the incident HCI and the formation of *hollow atoms* [1-6]. In particular, the so-called *potential sputtering* rather than the usual *kinetic sputtering* is presently attracting considerable interest [7] for its possible applications in technology related to delicate sputter cleaning, fabricating nano-structures or material modifications in nano-scale domain [8]. The field is also promising for its importance in understanding fundamental mechanism of highly charged ion interaction with solid surfaces [9]. The Si surface with hydrogen is a unique combination for the investigation of adsorption and desorption of molecules from semiconductor surfaces. Hydrogen on Si at low coverage forms monohydrate and keeps the Si surface protected from other contaminations. The characteristics of thermal desorption of hydrogen show interesting features [10] that have attracted more researches [11-14] on it. It is known that atomic hydrogen adsorbs readily on Si by saturating the dangling bonds and forming Si-H bonds, but the sticking co-efficient of molecular hydrogen is extremely low; as low as ~10^{-9} at room temperature [15]. It is likely, therefore, that the desorbed hydrogen from Si is mostly comprising of the molecular component. There are reports on the desorption studies of hydrogen from Si by a number of methods. Soukiassian et al. [11], in their scanning tunneling microscopy study, showed that atomic-scale desorption of hydrogen from Si(100)-(2×1) surface follows a power law with tunnel current in the STM where inelastic electron channels are more effective. Extensive studies on hydrogen desorption are carried out by Tok et al. [12]. Burgdörfer *et al*. [13] reported potential sputtering of protons by highly charged ions from relatively thick hydrocarbon layers where substrate properties can be neglected. Their theoretical investigation on the desorption yield as a function of charge states was based on the classical over-barrier model and they formulated a scaling law of the yield $Y \sim q^{4...6}$ and predicted a saturation yield with charge states. Kuroki et al. [14] carried out an experiment on the charge state dependence of potential sputtering of proton from hydrogen terminated Si(100) surface bombarded by Xe ions (kinetic energy ≤ 5 keV and q = 4 - 12) and found an enhancement of sputtering yield independent of the surface conditions as well as projectile incident angle on the surface.

From the reviews of the above works and considering potential importance of highly charged ion interactions with insulator surfaces, we feel more experimental investigations are necessary to shed light on the mechanism of strange phenomena occurring from the surface under highly charged ion-irradiation at low energy. With this idea, we report here an experimental investigation of the desorption of hydrogen atoms from a silicon surface induced by impact of highly-charged xenon ions. We find evidence for a considerable enhancement of the desorption rate as a function of the incident projectiles charge. To our knowledge the present report may be the first result on hydrogen atom (as compared to proton) desorption/sputtering due to HCI impact.

2. Experimental

The experiment was performed using the 14.5 GHz ECR ion source at the Ionenstrahl-Labor (ISL) of the Hahn-Meitner-Institut in Berlin [16]. The ion source provides projectiles with kinetic energies up to $20q$ keV, where q is the charge state of the projectile. Projectiles with low kinetic energies were transported by keeping the beam line at high negative potential and by decelerating the ions prior to the entrance of the target chamber, thereby keeping the target chamber at ground potential.

The ion beam entered the target chamber through an opening of 3 mm diameter and was directed onto a Si(100) target which was sputter-cleaned by ion bombardment for several hours prior to the measurements. Typical beam currents during the experiment were about 1 particle nA. The target was placed on a simple x-y-z-ϕ manipulator inside an ultra-high vacuum chamber (base pressure 1.5×10^{-10} mbar, and 4.7×10^{-10} mbar with the valve to the ion beam line open); it was rotated 45° with respect to the incident beam. A quadrupole mass spectrometer was used to check the composition of the background gas. The spectrum gives the partial pressures of residual gases present in the chamber. The major part of the spectrum consists of H^+, H_2^+, C^+, N^+, O^+, O_2^+, OH^+, H_2O^+, OH_3^+, CO^+ and CO_2^+ positive ions, which are attributed to H_2, H_2O, CO, CO_2, O_2, and N_2 molecules. Apart from these we also found signals from C^{2+} and O^{2+}. Estimated partial pressures of the dominant H_2 and H_2O components obtained from the spectrum are 1×10^{-10} mbar and 2×10^{-11} mbar, respectively.

Optical spectra resulting from the bombardment of Si(100) by Xe^{q+} ions were taken with an optical spectrograph and recorded with an intensified CCD camera having 756 × 581 pixels (pixel width and height 11 μm each). The spectrograph was equipped with 3 different gratings of 100 lines/mm, 300 lines/mm and 1200 lines/mm; with the 100 lines/mm grating it was possible to record a wavelength regime of up to 400 nm simultaneously. The observation angle was 90° with respect to the incident beam and 45° relative to the surface normal.

3. Results and Discussion

A typical spectrum recorded during the bombardment of Si(100) by 30 keV Xe^{q+} (q = 10, 18, 22) is displayed in figure 1. The prominent lines result from sputtered Si atoms, which leave the surface in an excited state. At first glance surprising is the occurrence of several hydrogen Balmer (Hα, Hβ) lines. In comparison with the lines from sputtered Si, a pronounced charge-state dependence of the hydrogen lines is observed. This is illustrated in Fig. 1 by comparing the spectra taken for different incident charge states q = 10, 18, and 22. It is quite apparent from the figure that the hydrogen line intensity increases strongly compared to the silicon lines. This behaviour becomes more evident from figure 2 that displays the ratio of the Hα line relative to the Si 252 nm line (open circles). A dramatic increase of that ratio by more than one order of magnitude is observed when the charge state is varied from q = 6 to 22. The results displayed in figures 1 and 2 provide evidence for enhanced desorption of hydrogen atoms by highly-charged ions of moderate energy. Sputtering of silicon atoms is not expected to be significantly influenced by the incident charge state according to the results obtained by Sporn *et al.* [17] for total desorption yields of Si induced by highly charged ions.

We have measured the desorbed hydrogen atoms by optical spectroscopy, which can only detect excited atoms. In this measurement process, complexity may arise by the fact that atoms desorbed from the surface in their ground state can be excited by secondary electron showers via gas-phase excitation. Also hydrogen (protons) desorbed by HCI interaction with surface could be neutralised in the gas-phase by secondary electrons to generate excited-state hydrogen. This is of course very unlikely, because electron capture is always related to three-body collisions requiring a second proton or hydrogen atom in the collision volume or the simultaneous emission of a photon (this is the radiative electron capture process, abbreviated as REC) to account for energy and momentum conservations during the electron capture. Such

consequences have been discussed by Liu *et al.* [18] for the desorption of alkali metal atoms from alkali halide surfaces. For desorption of hydrogen from Si, the cross-section for electron-stimulated desorption (ESD) process has been measured by a number of authors [19,20] and they found that the cross section of ESD is on the order of ~ 10^{-20} to 10^{-19} cm^2 when the incident primary electron energy is varied from 50 to 300 eV. We may assume that most of the secondary electrons liberated from Si as a result of highly charged Xe-ions impact remain at much lower energies, as discussed recently also by Tona *et al.* [21]. Approximately 10^5 fast electrons would be required for ESD of a single hydrogen atom (H) from Si using the surface atomic density and the above cross section. Considering a realistic electron energy-distribution, the corresponding number of protons (H^+) is expected to be much smaller. On this argument, we can neglect the ESD process induced by secondary electrons liberated from Si surface with the impact of highly charged Xe-ions at a working pressure in the range of 10^{-5} to 10^{-10} mbar. It can, therefore, be concluded that desorption of hydrogen atoms takes place as a result of primary process of the HCI interaction with Si surface. This includes of course atomic collision cascades (nuclear sputtering) [22], ion-induced electronic desorption processes as well as the possible influence of hot surface electrons on the degree of atomic excitation of desorbed particles [9].

In order to investigate the adsorption and desorption dynamics of the hydrogen atoms, we have performed a second experiment where hydrogen gas was admitted to the target chamber through a needle valve. Hydrogen gas was introduced into the target chamber to change the partial pressure of hydrogen from which the arrival rate of hydrogen could be known. This could facilitate the process of adsorption and desorption of hydrogen apart from hydrogen desorbed from Si at relatively clean condition. The elevated pressure measured with an ionisation gauge taking the correction factor for molecular hydrogen into account was 1×10^{-5} mbar and lasted for about 140 min. Spectra were taken immediately before and after the hydrogen gas was turned off. Figure 3 shows the time (fluence) dependence of the hydrogen Balmer (Hα) line when the target is irradiated with either a 30 keV Xe^{10+} or Xe^{18+} beam at current densities of 36 and 8.5 particle nA/cm^2, respectively. Here the Hα line intensity has been normalized to the incident ion intensity. It is evident that the hydrogen signal falls off with increasing fluence before it levels off at about 30-50% of its maximum value.

The hydrogen adsorption on the target surface is governed by the arrival rate of hydrogen molecules Φ_H multiplied by the constant sticking coefficient c_s and the removal rate of hydrogen atoms from the surface by sputtering (sputtering coefficient S_H). It is reasonable to assume that the sticking coefficient c_s is independent of the hydrogen coverage for less than a monolayer. The time dependence of the hydrogen coverage θ (in terms of the clean surface atom density) is, hence, determined by the rate equation [23-25]

$$\frac{d\theta}{dt} = -\frac{1}{n_s}(\Phi_+ S_H + \Phi_H c_s)\theta + \frac{\Phi_H c_s}{n_s} \qquad (1)$$

where Φ_+ is the incident ion flux density and $n_s = 1.18 \times 10^{15}$ atoms/cm^2 is the surface-atom density of silicon. At large times, $d\theta/dt \rightarrow 0$ and the equilibrium coverage θ_{eq} is given by

$$\theta_{eq} = \frac{\Phi_H}{\Phi_H + \frac{S_H}{c_s}\Phi_+} = \left(1 + \frac{\Phi_+ S_H}{c_s \Phi_H}\right)^{-1} \qquad . \qquad (2)$$

Eq. (1) has the general solution

$$\theta(t) = \frac{1}{\Phi_+ S_H + \Phi_H c_s}\left[\Phi_H c_s + \left[(\Phi_H c_s + \Phi_+ S_H)\theta_0 - \Phi_H c_s\right]\exp\left(-\frac{1}{n_s}(\Phi_+ S_H + \Phi_H c_s)t\right)\right], \qquad (3)$$

where $\theta_0 = \theta(t=0)$. Combining Eqs.2 and 3, we finally get

$$\theta(t) = \theta_{eq} + (\theta_0 - \theta_{eq})\exp\left(-\frac{\Phi_H c_s}{n_s \theta_{eq}} t\right) \qquad (4)$$

With the help of Eq. (4) it is possible to analyse the time dependence of the measured hydrogen signal, if we assume that the hydrogen Balmer line intensity is proportional to the time dependent coverage $\theta(t)$ by hydrogen. While the hydrogen coverage may in principle influence the excitation probabilities of desorbed atoms due to changes in the surface density of states, such an influence is expected to be small for highly excited n-states (n=3 in the present case) that do always have a considerable overlap with conduction-band states at small ion-surface distances.

Performing a non-linear least squares fit of Eq. 4 to the data, we obtain the unknown quantities $(\Phi_+ S_H + \Phi_H c_s)/n_s$ and θ_0/θ_{eq}. To eliminate the hydrogen flux contribution to the surface we are reminded that molecular hydrogen does not stick on a Si(100) surface [15]. The dominant contribution to the surface coverage, hence, stems from water molecules present in the residual gas. The flux density Φ_M of a particular molecule M to a surface is given as

$$\Phi_M = \frac{1}{4} n\bar{v} = \sqrt{\frac{p^2}{2\pi mkT}} \qquad (5)$$

where p is the partial pressure, k the Boltzmann constant, $T \approx 300$ K the temperature, and m is the molecular mass. Using the known partial pressure of water $p_{H2O} = 2\times10^{-11}$ mbar (see above) and taking into account that each water molecule carries 2 hydrogen atoms, we estimate a relevant flux density of hydrogen atoms $\Phi_H = 1.4 \times10^{10}$ cm^{-2}s^{-1}. We use this number together with a sticking coefficient c_s of unity in the analysis of the data shown in figure 3. For the sputtering yield we obtain from the Xe^{10+} data in figure 4, a value of $\Phi_+ S_H = (1.81 \pm 0.18) \times 10^{11}$ cm^{-2} s^{-1}. Using the known ion flux density of $\Phi_+ = 2.37 \times 10^{11}$ cm^{-2} s^{-1} we obtain, for 30 keV Xe^{10+} incident at 45 degrees, a sputtering yield $S_H = 0.76 \pm 0.08$ hydrogen atoms per incident ion. Similarly, from the Xe^{18+} data in figure 4, we obtain a value of $S_H = 2.2 \pm 0.4$ hydrogen atoms per incident ion. Here the error bars represent the statistical errors only, to which an absolute error of ± 30% has to be added. The trend, which is indicated by these numbers, is shown by the closed symbols in figure 4. These yields appear to be rather large, in particular, if we consider the low bombarding velocity and the inefficient kinetic energy transfer between silicon atoms, which constitute the major part of the collision cascade, and the hydrogen atoms at the silicon surface. This is further supported by a simulation based on the TRIM code [22] which yields $S_H = 0.018$ hydrogen atoms per incident Xe^{10+} ion for chemisorbed hydrogen. We therefore believe that the major mechanism for hydrogen desorption is *potential sputtering* induced by the high charge state of the incident Xe^{q+} ion, rather than *kinetic sputtering* within the binary collision model [22].

Figure 4 displays the absolute desorption yields derived from the results in figure 3 together with the relative photon-emission yields from figure 2 (i.e., the normalised H_α line intensity). Our plotted charge-state trend of the relative photon-emission yields due to H* production in Fig. 4 may be fitted by a $q^{2.6\pm0.2}$ dependence. It has to be kept in mind, however, that these relative yields are normalized to the Si* photon-emission yields and not to the projectile current. One cannot completely exclude a possible charge-state dependence of the Si* yield for our relative yields. Tona et al. [21] reported a $q^{1.4}$ charge-state dependence for sputtering of Si^+ ions at higher Xe projectile charge-states and a weak (roughly $q^{0.5}$) dependence for projectiles slightly above q=16. For q<9 Aumayr et al. found no q dependence at all [7]. Theoretical estimates using adiabatic ion-atom scattering-potentials in the local-density model

[26] point also to a very weak dependence ($q^{0.2}$) of the nuclear energy-loss cross-section and to the nuclear sputtering yield, respectively. Hence, when correcting our relative data for an assumed weak q-dependence ($q^{0.2\pm0.2}$) of the Si* production, we find an excited atomic hydrogen yield Y(H*) ~ $q^{2.8\pm0.3}$. This exponent is only somewhat lower than the one in the $q^{3.4}$ dependence found by Tona et al. [21] for H^+ emission. In this context, it can be stated that desorption/sputtering of protons and desorption/sputtering of excited hydrogen atoms need not to have the same *q*-dependence. Charge-state distributions of desorbed atoms depend on the surface-density-of-states as well as on the level structure of the desorbed atom.

Let us now consider the two data points (for q= 10 and 18) with solid symbols in Fig. 4. The values of S_H = 0.76 and 2.2 hydrogen atoms per incident ion exceed the absolute proton yields measured by other groups by about two orders of magnitude. This means neutral-particle ejection dominates the desorption process. Such a behaviour is common for many materials. It suggests that the charged-particle yield $Y(H^+)$ may be written as

$$Y(H^+, p) = f(H^+, p) \times \left(Y(H^+, p) + Y(H^0, p) + Y(H^-, p)\right) \approx f(H^+, p) \times Y(H^0, p), \qquad (6)$$

where $f(H^+)$ is the small positive charge-state fraction and the parameter p shall indicate any possible dependence on the projectile state (speed, charge state, incident angle, …). One may immediately guess that an interpretation of $Y(H^+)$ will be difficult, because it is a product of the total sputtering yield and the positive charge-state fraction which both depend on the projectile properties. We assume furthermore that the hydrogen exited-state population discussed above is also only a small fraction of the total sputtering yield.

Comparison of the trends given by the solid (absolute desorption yields) and the open symbols (relative H-alpha light intensity) allows to extract a rough charge-state dependence of the excited-state fraction $f(H^*) = Y(H^*)/Y(H^0)$. From the ratio of the two types of data we derive a $q^{1.0\pm0.8}$ dependence. Correcting for the assumed weak Si* dependence as above, we estimate $f(H^*) \sim q^{1.2\pm0.8}$. Using $f(H^+) \cong Y(H^+)/Y(H^0) = f(H^*)\cdot Y(H^+)/Y(H^*) \sim q^{1.8\ \pm0.9}$, the positive charge-state fraction $f(H^+)$ might be even slightly more sensitive to the projectile charge state than the excited-state fraction f(H*).

The solid line of fig.4 displays the total potential projectile energy from Hartree-Fock-Slater calculations arbitrarily divided by 185 eV to fit the data. As can be seen there is reasonable agreement between experimental data and the potential energy curve. In the desorption

process, mainly hydrogen atoms from the topmost surface layers come into play. Since charge-state equilibration of the projectile appears up to a few layers below the surface, only a certain fraction of the potential energy can be converted into desorption. Therefore we can state, the experimental desorption yield is found to be proportional to the potential energy of the projectile. Furthermore, this proportionality points to very unspecific excitation processes being not sensitive to the projectile level-structure.

4. Conclusion

In conclusion, while the sputtering of silicon atoms by highly-charged ions of medium energy (30-100 keV) appears to be dominated by the *kinetic sputtering* mechanism, we believe to have found evidence that the desorption of surface hydrogen atoms is significantly influenced by *potential sputtering*. Previous studies [13,14,21] (measuring secondary ion emission) have mainly focussed on proton desorption from hydrogen terminated or hydrocarbon covered Si surfaces and reported a scaling of the proton sputtering yield with charge state q as q^n with $3 < n < 5$. In this work two different experimental approaches were used:

(a) Hydrogen Balmer-alpha light emission from desorbed (excited) hydrogen atoms (relative to light emission from sputtered excited silicon atoms) is studied as a function of Xe^{q+} projectile charge state $6 \leq q \leq 22$.

(b) The dependence of the hydrogen Balmer alpha line intensity on ion fluence was determined for two different projectile charge states (after hydrogen was admitted to the chamber for several hours). Using a model for the time/fluence dependence of the hydrogen coverage and several assumptions (e.g. on sticking coefficients for H_2 and H_2O molecules on Si) sputtering yields of 0.76 H atoms per Xe^{10+} ion and 2.2. H-atoms per Xe^{18+} ion were determined. These sputtering yields should be compared to the proton yields reported [21] (typically 10^{-3} protons/Xe^{12+} ion and 0.8 protons/Xe^{50+} ions). Such a large difference between secondary ion emission and neutral sputtering yield is common in literature and shows the importance of neutral particle desorption due to potential sputtering. This enhanced desorption yield might also have some consequences for applications that rely on low surface-hydrogen concentrations.

References

[1] H.J. Andrä, Nucl. Instr. Meth. B 43 (1989) 306.

[2] L. Folkerts, R. Morgenstern, Europhys. Letters 13 (1990) 377.

[3] F.W. Meyer, S.H. Overbury, C.C. Havener, P.A. Zeijlmans van Emmichoven, D.M. Zehner, Phys. Rev. Letters 67 (1991) 723.

[4] J. Limberg, S. Schippers, R. Hoekstra, R. Morgenstern, H. Kurz, F. Aumayr, HP. Winter, Phys. Rev. Letters 75 (1995) 217.

[5] F. Aumayr, HP. Winter, Comm. At. Mol. Phys. 29 (1994) 275.

[6] N. Stolterfoht, D. Niemann, M. Grether, A. Spieler, A. Arnau, C. Lemell, F. Aumayr, HP. Winter, Nucl. Instr. Meth. Phys. Res. B 124 (1997) 303

[7] F. Aumayr, P. Varga, H.P. Winter, Int. J. Mass Spec. 192 (1999) 415

[8] T. Schenkel, M. Schneider, M. Hattass, M.W. Newman, A.V. Barnes, A.V. Hamza, D.H. Schneider, R.L. Cicero, C.E.D. Chidsey, J. Vac. Sci. Technol. B 16 (1998) 3298.

[9] G. Schiwietz, K. Czerski, M. Roth, F. Staufenbiel, P.L. Grande, Nucl. Instr. Meth. B 225 (2004) 4.

[10] Z. Hu, A. Biedermann, E. Knoese, T.F. Heinz, Phys. Rev. B 68 (2003) 155418.

[11] L. Soukiassian, A.J. Mayne, M. Carbone, G. Dujardin, Phys. Rev.B 68 (2003) 035303.

[12] E.S. Tok, J.R. Engstrom, H.C. Kang, J. Chem. Phys. 115 (2001) 6550; E.S. Tok, J.R. Engstrom, H.C. Kang, J. Chem. Phys. 118 (2003) 3294;E.S. Tok, S.W. Ong, H.C. Kang, J. Chem. Phys. 120 (2004) 5424.

[13] J. Burgdörfer, Y. Yamazaki, Phys. Rev.A 54 (1996) 4140.

[14] K. Kuroki, N. Okabayashi, H. Torii, K. Komaki, Y. Yamazaki, Appl. Phys. Letts. 81 (2002) 3561.

[15] P. Bratu and U. Höfer, Phys. Rev. Letts. 74 (1995) 1625.

[16] B. Martin, M. Grether, R. Köhrbrück, U. Stettner, H. Waklmann, *Proc. 11th Int. Workshop on Electron Cyclotron Resonance Ion Sources (ECR)*, Groningen (1993), p. 188.

[17] M. Sporn, G. Libiseller, T. Neidhart, M. Schmid, F. Aumayr, HP. Winter, P. Varga, M. Grether, D. Niemann and N. Stolterfoht, Phys. Rev. Letters 79 (1997) 945; P. Varga, private communication and invited talk presented at the *17th international conference on atomic collisions in solids*, Beijing, July (1997).

[18] D. Liu, N. Seifert, D.J. McClure, A.V. Barnes, R.G. Albridge, N.H. Tolk, D. Russel, Phys. Rev. B 47 (1993) 1553.

[19] K. Ueda, Jpn. J. Appl. Phys. 33 (1994) 1524.

[20] M.M. Albert, N.H. Tolk, Phys. Rev. B 63 (2000) 035308.

[21] M. Tona, K. Nagata, S. Takahashi, N. Nakamura, N. Yoshiyasu, M. Sakurai, C. Yamada, S. Ohtani, Surf. Sci. 600 (2006) 124.

[22] J.F. Ziegler, J.P. Biersack, *The Stopping and Range of Ions in Solids*, Pergamon: New York (1985).

[23] R. Kelly, C.B. Kerkdijk, Surf. Sci. 46 (1974) 537.

[24] D. Ghose, U. Brinkmann, R. Hippler, Surf. Sci. 327 (1995) 53.

[25] D. Ghose, R. Hippler, In: *Luminescence in Solids* (D.R. Vij, Ed), Plenum Press: New York, (1998) pp. 189.

[26] P.L. Grande and G. Schiwietz (private communication, 2005). Actual calculations were similar to the ones that have lead to the well-accepted averaged ZBL potential fit [22].

Figure Captions:

Figure 1: Light-emission spectrum following 30 keV Xe^{q+} (q = 10, 18, and 22) bombardment of Si(100). The wavelengths of some optical transitions from neutral silicon and neutral hydogen (Hα, Hβ) are indicated. Note the pronounced increase of the Hα and Hβ lines with increasing projectile charge.

Figure 2: Measured ratio of the Hα line to the Si(252 nm) line (open circles) versus incident charge state q. Note that the ratios have not been corrected for a dependence of the desorption rate on the ion beam current.

Figure 3: Fluence dependence of the hydrogen Balmer (Hα) line after hydrogen was admitted to the chamber for several hours (see text).

Figure 4: The desorption yield of atomic hydrogen deduced from figure 3 (closed symbols) versus incident charge state q. Also shown is the (normalized) ratio of the Hα line to the Si(252 nm) line (open circles). The solid curve represents the charge-state dependence of the *potential energy* of the projectile (see text).

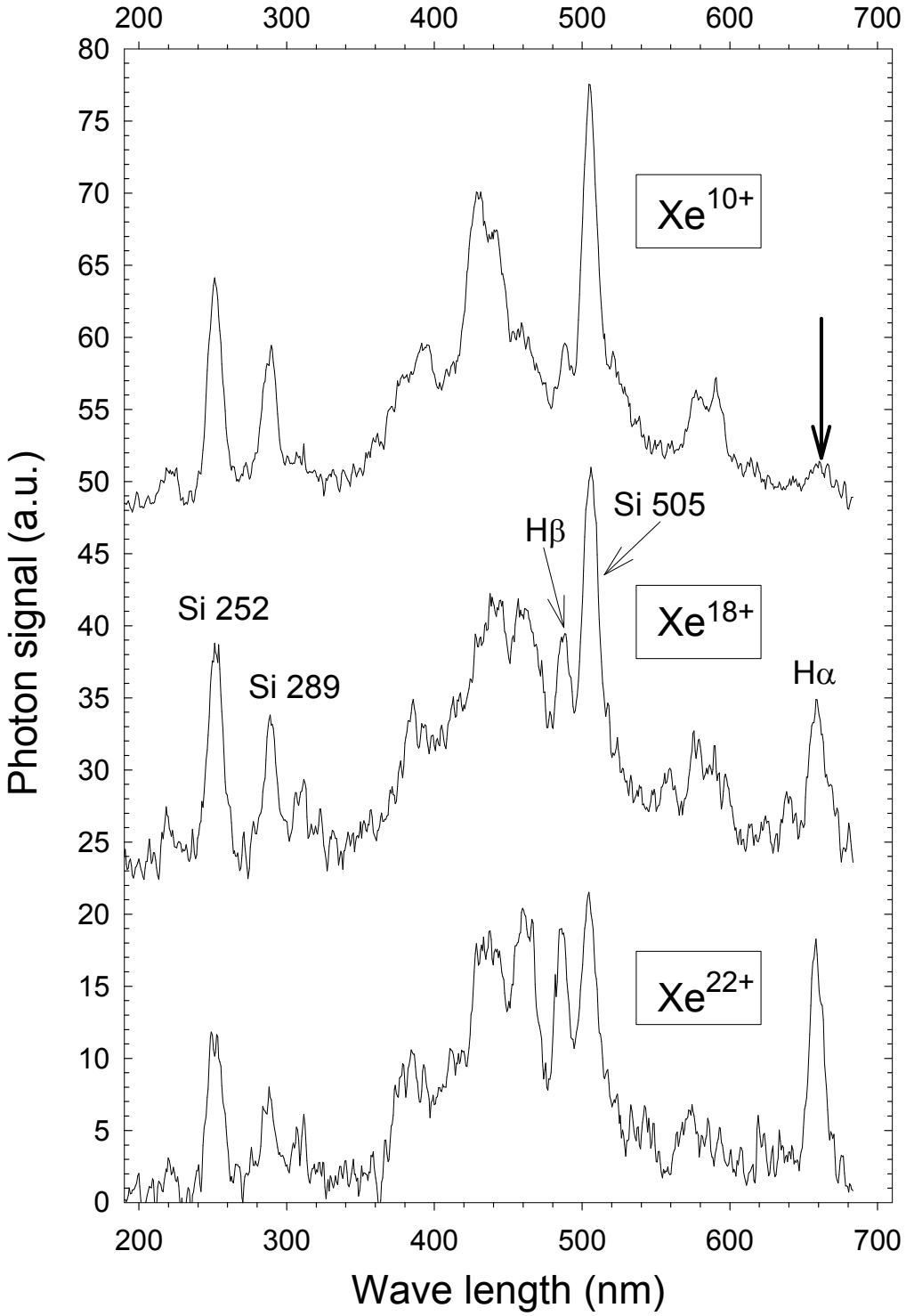
Photon signal (a.u.)
Wave length (nm)
Xe10+
Xe18+
Xe22+
Si 252
Si 289
Hβ
Si 505
Hα

Figure 1

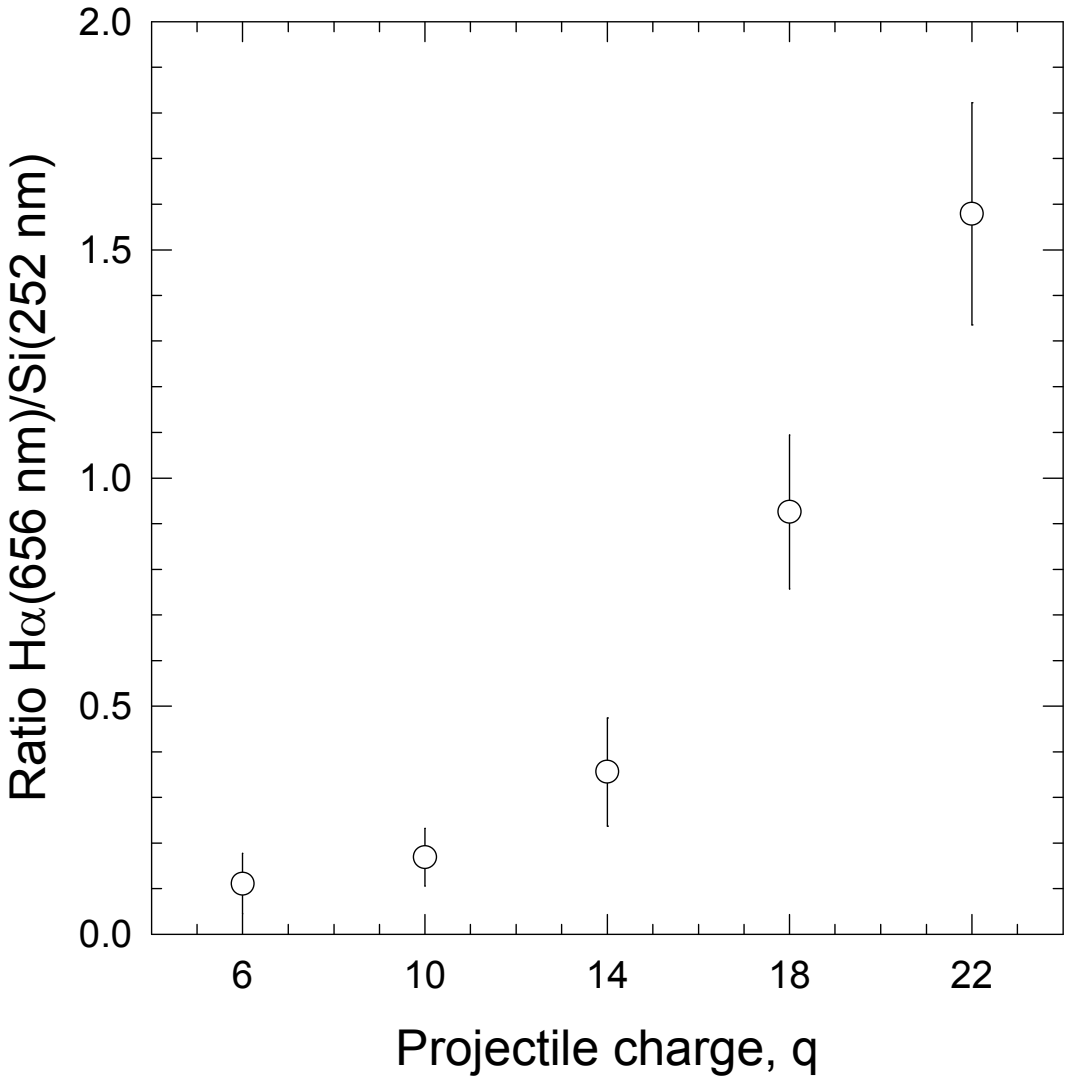

Figure 2

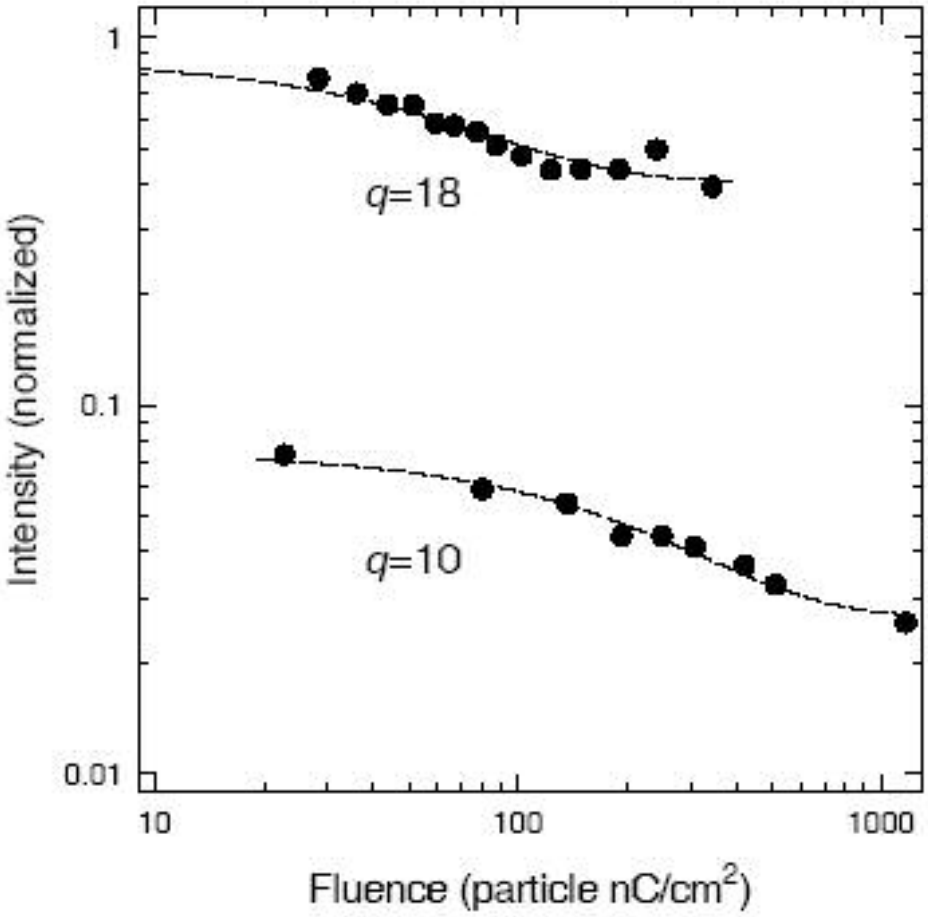
1
0.1
0.01
Intensity (normalized)
q=18
q=10
10
100
1000
Fluence (particle nC/cm2)

Figure 3

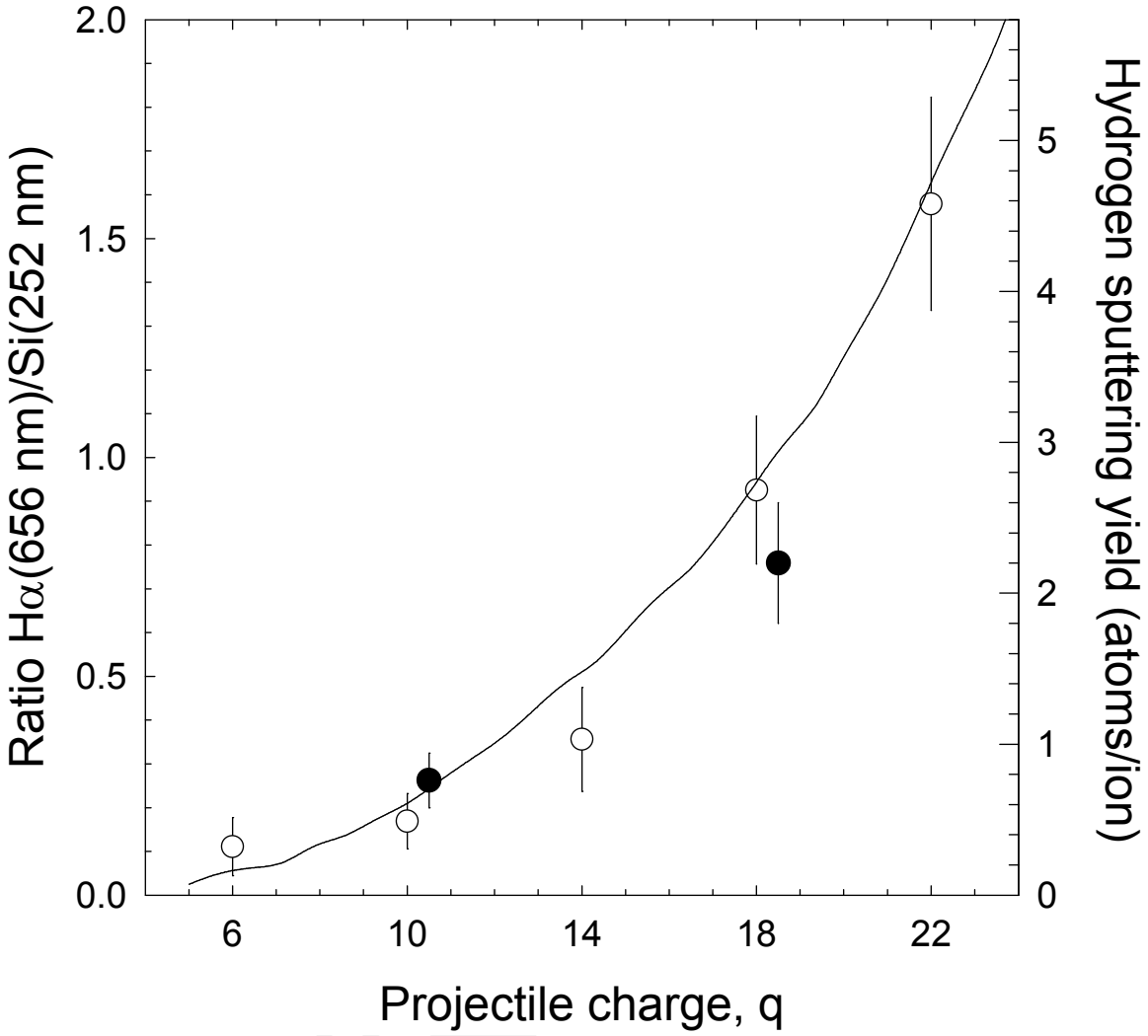
Ratio Hα(656 nm)/Si(252 nm)
Hydrogen sputtering yield (atoms/ion)
Projectile charge, q
2.0
1.5
1.0
0.5
0.0
5
4
3
2
1
0
6
10
14
18
22

Figure 4